

EXPERIMENTAL AND ANALYTICAL INVESTIGATION ON BUCKLING OF
THE COMPOSITE STIFFENED PANEL UNDER COMPRESSION AND SHEAR

Tong Xianxin, Guan Dexin, Gao Zhiheng
Li Xinxiang, Fan Yin'an, Zhang A'ying
Aircraft Strength Research Institute, CAE
710061 P. O. Box 86, Xi'an, Shaanxi, China

Abstract

A new test technique and an improved "finite strip element method" for buckling analysis of composite stiffened panel under combination of compression and shear are presented.

A special auxiliary device has been developed on base of a clever resolution of force. the buckling test of rectangular panel under combined loads of compression and shear can be made by use of this device even on a universal compressive test machine. It is convenient for engineering practice. The test cost can be reduced considerably as compared with that of traditional "torsion/bending of box".

In the finite strip element method, two dimensional complex exponential buckling displacement functions for analysis of a typical strip are simplified. As a result, the complex eigenvalue problem is transformed into real one. Thus good calculation efficiency and convergence can be achieved. And a general program has been developed.

The buckling tests of four composite stiffened panels under compression and shear on a type of universal test machine with this device have been made successfully. The numerical results from the program are in good agreement with the test data.

1. Introduction

The critical design of the stiffened panels in aircraft structures is their stability design under combination of compression and shear. As we know, it is difficult to apply the combinative load on a single panel uniformly and simultaneously. "torsion/bending of box" composed of four panels, a traditional way, is usually used in engineering. It needs to make 3~4 box tests to obtain a reliable datum. For the composite panel, that kind of test is too expensive to do.

In this paper a new test technique and the correlative device will be recommended. [1] By use of this special auxiliary device the buckling test on single panel under combination of

compression and shear can be made even on a universal compressive test machine. The buckling tests of four composite stiffened panels in the specified ratio of shear to compression have been made for designing a fin of a type of aircraft. [2] The test results show that the load is well-distributed and simultaneous, and the ratio of shear to compression accords with the specified value well.

An improved "finite strip element method" has been developed as well. [3] The stiffness matrix of strip element is derived by use of an analytical method. As to consider the buckling mode of panel under compression and shear, two dimensional complex exponential buckling displacement functions are used. Thus the stiffness matrix should be complex in general and it adds even more complexity to the buckling analysis. Then a simplified scheme for the complex functions is presented. As a result, the complex expressions of the stiffness matrix are transformed into real one. Thus good calculation efficiency and convergence can be achieved. A general program has been developed. [4] The numerical results of the four composite panels mentioned above are in good agreement with the test data.

II. A New Test Technique and Special Device[1]

As shown in Fig. 1 and 2, the specimen is installed slopingly in the special device placed on a universal compressive test machine. The ends of specimen are connected with a pair of main loading blocks. The sides of specimen are connected with the shearing blocks. The shearing blocks are connected with the supports as well. The applied load from test machine is resolved into the desired combinatory compression-shear (N_x and N_{xy}) at ends of the specimen and shear (N_{xy}) at sides of the specimen. The loadings are automatically compatible. The ratio (N_{xy}/N_x) can be simply controlled by changing the slope angle α (the specimen end line to horizon). The applied load can be spreaded effectively, so compression and shear loaded on the boundaries of specimen can be well-distributed. The compressive and shear deformations of specimen may not be restricted. The supporting conditions at boundaries of specimen can be imitated in engineering. Test shows that loading of test machine is not obstructed.

A self-balancing system is designed to remove the transversal loads (N_y) on the sides of the specimen. And axles fixed at the secondary loading blocks can move in direction x and y smoothly. Only the shear component of the applied load can pass on both sides of the specimen.

The roller are placed under (or upper) the loading blocks, supports and levers in order that the inplane deformations of the specimen are not restricted.

According to the design principle of the device, the sloping angle α is determined by the ratio of shear to compression, as follows

$$A = N_{xy}/N_x \quad (2-1)$$

$$\alpha = \arctan(A)$$

where

- N_x the compression per unit width
- N_{xy} the shear per unit width
- α the sloping angle of ends of specimen to the platform of the test machine

Knowing the total compressive load P_x and A , the applied load P of the test machine can be obtained by use of the following fomula

$$P = P_x \left(1 + \frac{a}{b} A \right) \sqrt{1 + A^2} \quad (2-2)$$

where

- b the width of end loaded compression and shear
- a the length of side loaded shear
- $P_x = bN_x$

III. An Improved Finite Strip Element Method^[3]

The analytical method for the buckling of stiffened composite panels under compression and shear is extended by the method in Ref. [5] and Ref. [6].

It is the key to analyse the stiffness matrix of a typical strip element. It can be resolved by the analytical method. For the symmtric laminate, the Donnell's differential equilibrium equations of a strip element can be written as

$$\begin{aligned} & A_{11}u_{,xx} + 2A_{16}u_{,xy} + A_{66}u_{,yy} + A_{16}v_{,xx} + A_{26}v_{,yy} \\ & + (A_{12} + A_{66})v_{,xy} = 0 \\ & A_{16}u_{,xx} + (A_{12} + A_{66})u_{,xy} + A_{26}u_{,yy} + A_{66}v_{,xx} \\ & + A_{22}v_{,yy} + 2A_{26}v_{,xy} = 0 \quad (3-1) \\ & D_{11}w_{,xxxx} + 4D_{16}w_{,xxyy} + 2(D_{12} + 2D_{66})w_{,xyxy} \\ & + 4D_{26}w_{,xyyy} + D_{22}w_{,yyyy} + \bar{N}_x w_{,xx} \\ & + \bar{N}_y w_{,yy} + 2\bar{N}_{xy} w_{,xy} = 0 \end{aligned}$$

It is very difficult to solve the above equations exactly. Generally "the inverse method" can be used. A proper buckli-

ing displacement functions are selected as follows

$$\begin{aligned} w &= \sum_{j=1}^4 W_j e^{i\alpha_j y} e^{i\beta_j x} \\ u &= \sum_{j=1}^4 U_j e^{i\alpha_j y} e^{i\beta_j x} \\ v &= \sum_{j=1}^4 e_j e^{i\alpha_j y} e^{i\beta_j x} \end{aligned} \quad (3-2)$$

where

$i = \sqrt{-1}$, $\beta = \pi/\lambda$, λ is the buckling half-wavelength, the α_j are the undetermined constants.

Substituting Eq. (3-2) into Eq. (3-1), the fourth order polynominals of α_j relating to the u, v and w can be obtained. Then α_j are determined.

Note that the polynominals of α_j have real coefficients and hence roots of α_j must be either real or conjugate complex. And the undetermined displacements U_j, V_j and W_j are independent, any j th item of displacement functions corresponding to α_j should satisfy Eq. (3-1). The correlative factor between U_j and V_j can be formulated. As above characteristics, the displacement functions are simplified as follows

For the case of complex conjugate roots $\alpha_j = r + mi$, $\alpha_{j+1} = r - mi$

$$\begin{aligned} u_{i,j+1} &= B_{30}[\xi(sc)_1 + \eta(cs)_1] + B_{40}[\xi(ss)_1 - \eta(cc)_1] \\ & + B_{10}[\xi(cc)_1 + \eta(ss)_1] + B_{20}[\xi(cs)_1 - \eta(sc)_1] \\ & + \{B_{30}[\xi(ss)_1 - \eta(cc)_1] - B_{40}[\xi(sc)_1 + \eta(cs)_1] \\ & + B_{10}[\xi(cs)_1 - \eta(sc)_1] - B_{20}[\xi(cc)_1 + \eta(ss)_1]\}i \\ v_{i,j+1} &= B_{10}(cc)_1 + B_{20}(cs)_1 + B_{30}(sc)_1 + B_{40}(ss)_1 \\ & + [B_{10}(cs)_1 - B_{20}(cc)_1 + B_{30}(ss)_1 - B_{40}(sc)_1]i \\ w_{i,j+1} &= B_1(cc) + B_2(cs) + B_3(sc) + B_4(ss) \\ & + [B_1(cs) - B_2(cc) + B_3(ss) - B_4(sc)]i \quad (3-3) \end{aligned}$$

For the case of real roots $\alpha_j = r$

$$\begin{aligned} u_j &= [B_{10}' \cos(ry) + B_{20}' \sin(ry)]\xi \\ & + [B_{10}' \sin(ry) - B_{20}' \cos(ry)]\xi i \\ v_j &= [B_{10}' \cos(ry) + B_{20}' \sin(ry)] \\ & + [B_{10}' \sin(ry) - B_{20}' \cos(ry)]i \\ w_j &= [B_1' \cos(ry) + B_2' \sin(ry)] \\ & + [B_1' \sin(ry) - B_2' \cos(ry)]i \quad (3-4) \end{aligned}$$

where

- $(cc) = \text{ch}(my) \cos(ry)$
- $(cs) = \text{ch}(my) \sin(ry)$
- $(sc) = \text{sh}(my) \cos(ry)$
- $(ss) = \text{sh}(my) \sin(ry)$

$B_{10} \sim B_{40}, B_{10}' \sim B_{20}', B_1 \sim B_4, B_1' \sim B_2'$ are transformed undetermined displacement coefficients u, v and w respectively. ξ, η are constants related to u and v .

Next the stiffness matrix of the strip element will be for-

mulated. According to variational derivation,^[7] the generalized forces are determined as Q_y, M_y, N_y and N_{xy} corresponding to the generalized displacements w, θ, v and u at sides of the strip^[8]

$$\{d\} = \begin{Bmatrix} w_s \\ \theta_s \\ v_s \\ u_s \end{Bmatrix} = \begin{Bmatrix} w + y_0 w_{,y} \\ w_{,y} \\ v - z_0 w_{,y} \\ u - y_0 v_{,x} - z_0 w_{,x} \end{Bmatrix} \quad (3-5)$$

$$\{f\} = \begin{Bmatrix} Q_{ys} \\ M_{ys} \\ N_{ys} \\ N_{xys} \end{Bmatrix} = \begin{Bmatrix} Q_y \\ M_y + y_0 Q_y - z_0 N_y \\ N_y - y_0 N_{xy,x} \\ N_{xy} \end{Bmatrix} \quad (3-6)$$

where the symbols with subscript "s" indicate the quantities at the common intersection line of neighbouring strips, the others without "s" represent the quantities in the reference plane of strip. The y_0 and z_0 are the offsets of common intersection from the side in reference plane (See Fig. 11). And

$$\begin{aligned} Q_y &= -2D_{16}W_{,xxx} - (D_{12} + 4D_{66})W_{,xxy} \\ &\quad - 4D_{26}W_{,xyy} - D_{22}W_{,yyy} \\ M_y &= -D_{12}W_{,xx} - D_{22}W_{,yy} - 2D_{26}W_{,xy} \\ N_y &= A_{12}u_{,x} + A_{22}v_{,y} + A_{26}(u_{,y} + v_{,x}) \\ N_{xy} &= A_{16}u_{,x} + A_{26}v_{,y} + A_{66}(u_{,y} + v_{,x}) \end{aligned} \quad (3-7)$$

If the $\{d\}$ and $\{f\}$ are in complex form, they can be written as

$$\begin{aligned} \{d_c\} &= \{d_r\} + \{d_m\}i \\ \{f_c\} &= \{f_r\} + \{f_m\}i \end{aligned}$$

where subscripts "c", "r" and "m" represent the complex, real and imaginary part respectively.

Assume the stiffness matrix in complex form as

$$[s_c] = [s_r] + [s_m]i$$

as the definition of stiffness

$$\{f_c\} = [s_c]\{d_c\}$$

then

$$\begin{aligned} \{f_r\} &= [s_r]\{d_r\} - [s_m]\{d_m\} \\ \{f_m\} &= [s_m]\{d_r\} + [s_r]\{d_m\} \end{aligned}$$

in matrix form

$$\begin{Bmatrix} f_r \\ f_m \end{Bmatrix} = \begin{bmatrix} s_r & -s_m \\ s_m & s_r \end{bmatrix} \begin{Bmatrix} d_r \\ d_m \end{Bmatrix} \quad (3-8)$$

Hence, by Eq. (3-3)~eq. (3-7), the generalized displacements and forces can be expressed in rearranged form, respectively

$$\begin{aligned} \{d_s\} &= \begin{Bmatrix} d_r \\ d_m \end{Bmatrix} \\ \{f_s\} &= \begin{Bmatrix} f_r \\ f_m \end{Bmatrix} \end{aligned}$$

and it has been found

$$\{d_s\} = \begin{bmatrix} x_{A0} & x_{B0} \\ x_{B0} & -x_{A0} \end{bmatrix} \{B\} = [x]\{B\} \quad (3-9)$$

$$\{f_s\} = \begin{bmatrix} y_A & y_B \\ y_B & -y_A \end{bmatrix} \{B\} = [y]\{B\} \quad (3-10)$$

where $\{B\}$ are "equivalent undetermined displacement coefficients". It should be pointed out that $\{B\}$ are functions of x only. And $[x]$ and $[y]$ are functions of y .

As the definition of stiffness and Eq. (3-9) and Eq. (3-10), the stiffness matrix of a strip element in rearranged form are obtained

$$\begin{aligned} [S] &= [y][x]^{-1} \\ &= \begin{bmatrix} [y_A][x_A] + [y_B][x_B] & -[y_B][x_A] + [y_A][x_B] \\ [y_B][x_A] - [y_A][x_B] & [y_A][x_A] + [y_B][x_B] \end{bmatrix} \end{aligned} \quad (3-11)$$

where

$$\begin{aligned} [x_A] &= ([x_{A0}] + [x_{B0}][x_{A0}]^{-1}[x_{B0}])^{-1} \\ [x_B] &= ([x_{B0}] + [x_{A0}][x_{B0}]^{-1}[x_{A0}])^{-1} \end{aligned}$$

As compared with Eq. (3-8), the real part and imaginary part of the complex stiffness matrix are

$$\begin{aligned} [S_r] &= [y_A][x_A] + [y_B][x_B] \\ [S_m] &= [y_B][x_A] - [y_A][x_B] \end{aligned} \quad (3-12)$$

IV. Test and Analysis^[2]

Buckling tests of four composite stiffened panels under compression and shear on a type of universal compression test machine with this auxiliary device have been made.

The specimen sketch is shown in Fig. 3. There are four T-shape stiffeners and two ribs in the panel. The pitch between neighbouring stiffeners is 100mm, The pitch between two ribs is 300mm. Both length and width of the panel are 380mm.

The specimens are made of Graphite/Epoxy (T300/LWR-1) and properties of lamina are

$$\begin{aligned} E_{11} &= 142.4 \text{ GPa}, \quad E_{22} = 10.5 \text{ GPa}, \quad G_{12} = 4.9 \text{ GPa}, \\ \nu_{12} &= 0.3. \end{aligned}$$

The thickness of a lamina is 0.125mm. The stacking sequences are

Plate (skin)	[45/-45/0/45/-45/90]s
Stand-flange of stiffener	[-45/45/0/45]s
Lay-flange of stiffener	[-45/45/0/45]
Rib	[-45/45/0/45]s

Two of the specimens, 1-1 and 1-2 are made in the curing process; others, 2-1 and 2-2, are made in the secondary bonding process.

The nominal ratio between shear and compression is specified as

$$A = N_{xy}/N_x = 1$$

hence, the slopping angle of the specimen end to platform of

test machine is

$$\alpha = 45^\circ$$

if P_x is specified, the applied load of test machine is

$$P = \sqrt{2} P_x$$

In order to examine the distribution of loads in the specimen and determine the buckling load, the strains and deflections of specimens were measured. And the buckling model of specimen was displayed by morie photograph. The measured points of strain gauges and deflection are shown in Fig. 4.

The strain data were recorded and processed by micro-computer.

The test data-processing results of N_{xy}/N_x at measured points are listed in Table 2. The test buckling load and the comparison with analytical value are listed in Table 1.

The average test data of all measured points in plate are compared with the calculation values of shear and compression in Fig. 8 and Fig. 9, respectively.

The strains in the middle plane of plate and stand-flange of stiffener with applied loads are shown in Fig. 5 and Fig. 6.

The deflections of plate with applied load are shown in Fig. 7.

In analysis for the specimen, the buckling load is computed by the general program^[4] with the improved finite strip element method. The analytical buckling load and half-wave-length are

$$N_{x1} = 49.17 \text{ N/mm} \quad (\text{plate})$$

$$N_{xy1} = 63.31 \text{ N/mm} \quad (\text{plate})$$

$$\lambda = 150 \text{ mm.}$$

then the load of test machine at buckling should be

$$\begin{aligned} P_{cr} &= 2\sqrt{2} P_x = 2\sqrt{2} \times 63.31 \times 380 \\ &= 68049.5 \text{ N} = 68.05 \text{ kN} \end{aligned}$$

It is noticed that compressions on each type of strip elements are different. The load distribution is calculated by use of an engineering calculation

$$N_{x1}/N_x = 0.777 \quad (\text{for plate})$$

$$N_{x2}/N_x = 1.048 \quad (\text{for lay-flange with plate})$$

$$N_{x3}/N_x = 0.5295 \quad (\text{for stand flange})$$

the design ratios between shear and compression should be

$$(N_{xy}/N_x)_1 = 1.287 \quad (\text{for plate})$$

$$(N_{xy}/N_x)_2 = 0.9599 \quad (\text{for lay-flange with plate})$$

V. Conclusions

Test results show that compression and shear in plate of panels are well-distributed, and accord with the calculation. The test ratios between shear and compression in plate are in good agreement with the specified value. The transversal compressive load at sides of panel are removed effectively. So, the new test technique and the device are successful. And it is convenient for engineering practice. Compared with the traditional way, "torsion/bending of box", the test cost will be reduced considerably.

The numerical results of buckling load of specimens are in good agreement with test data. It shows that the proposed finite strip element method is available. The improved scheme makes the complex eigenvalue problem become real eigenvalue problem. Thus good calculation efficiency and convergence can be achieved.

References

- [1] Tong Xianxin, Gao Zhiheng, Guan Dexin, Zhang A'ying, Li Xinxiang and Fan Yin'an, "The Summarization of Experimental Investigations on the Method for Panels under Combination of Compression and Shear", Research Report of ASRI-CAE, Oct., 1990.
- [2] Tong Xianxin, Guan Dexin, Gao Zhiheng, Fan Yin'an, Li Xinxiang, Zhang A'ying, "Experimental and Analytical Investigations of Composite Stiffened Panels of a Fin under Compression and Shear", Research Report of ASRI-CAE, Dec., 1990.
- [3] Tong Xianxin, Li Xinxiang, "Buckling Analysis of Flat Stiffened Composite Panels under Compression and Shear", Research Report of ASRI-CAE, May, 1989.
- [4] Li Xinxiang, Tong Xianxin, "The Finite Strip Element Method Program BCP of Buckling Analysis for Composite Stiffened Panels under Compression and Shear", Research Report of ASRI-CAE, Dec., 1989.
- [5] Tong Xianxin, B. Geier, K. Rohwer, "Buckling Analysis of Discretely Stiffened Composite Curved Panels under Compression and Shear", Applied Mathematics and Mechanics, Vol. 7, No. 4, Apr., 1986.
- [6] A. V. Viswanathan, M. Tamkuni and L. L. Baker, "Elas-

tic Stability of Laminated, Flat and Curved, Long Rectangular Plates Subjected to Combined Inplane Loads”, NASA CR-2330.

[7] B. Geier, “Energy—based Task Formulations for Buckling Problems of Laminated Composite Shells”. Z. Flugwiss. 10, 215—227, 1986.

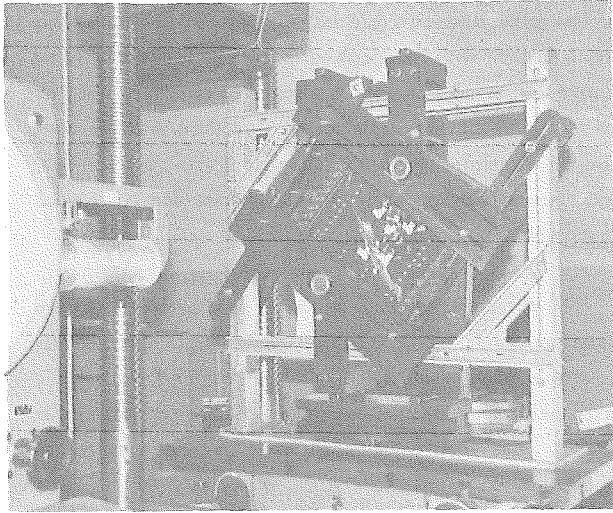


Fig. 1 Unloaded test device with crushing specimen and test machine

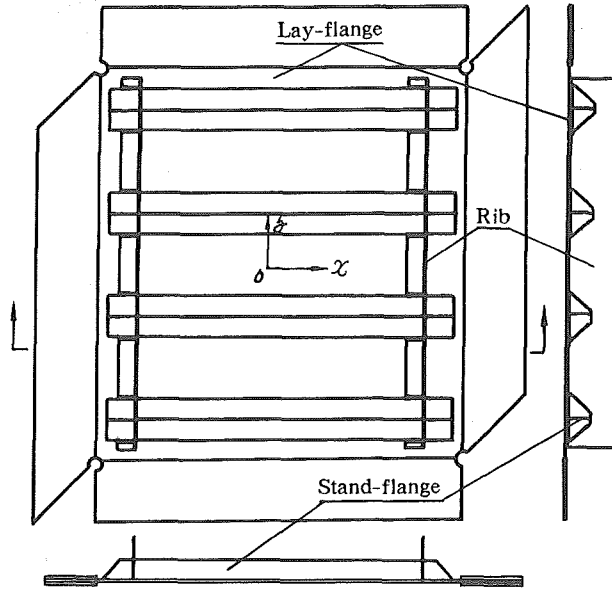


Fig. 3 Specimen sketch

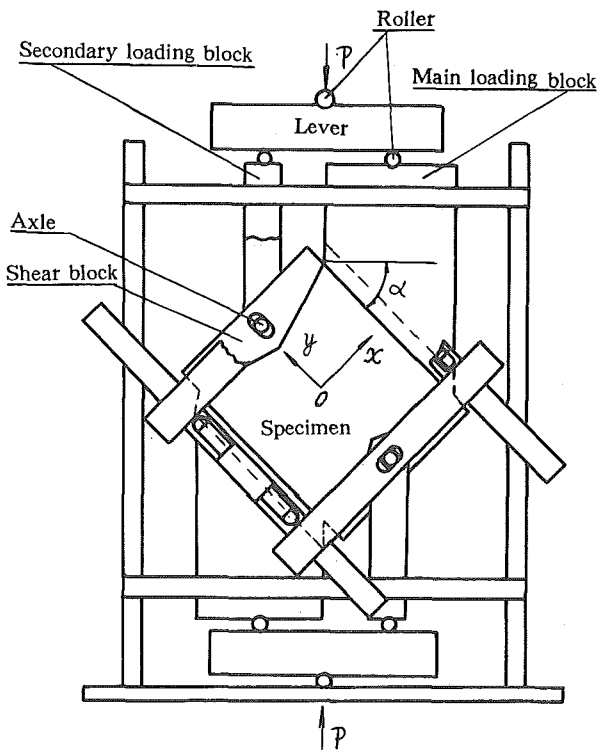
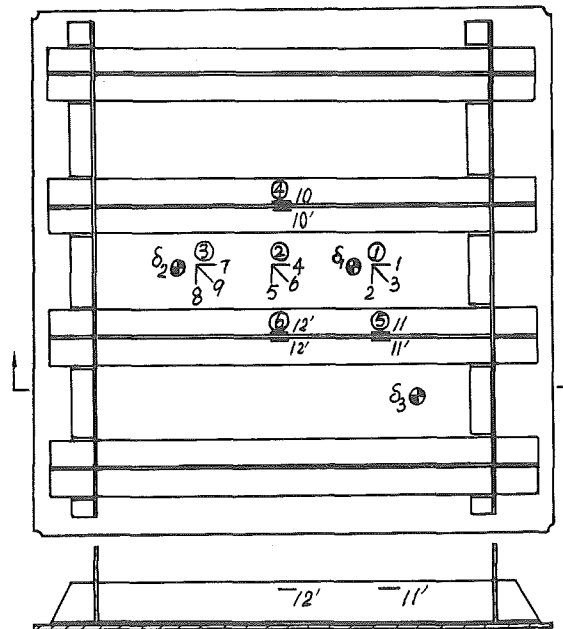


Fig. 2 Test device sketch



The number in “○” is the order of straingauges
 “⊕” is the point for measured deflection

Fig. 4 Location of measured points of strain and deflection

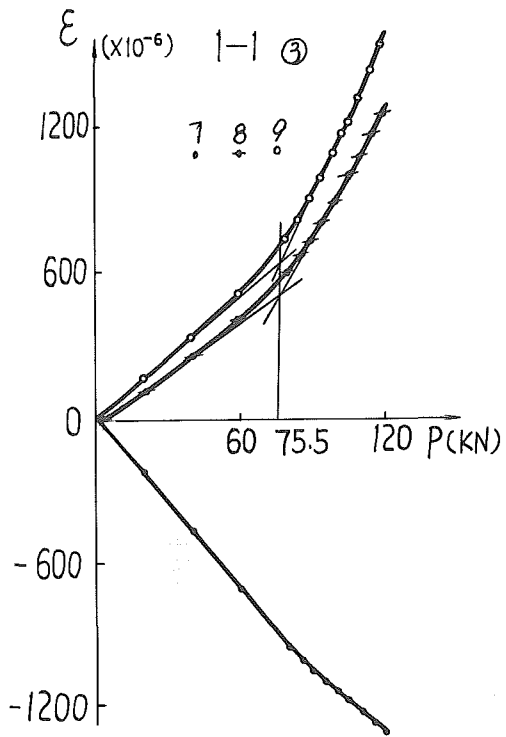


Fig. 5. a Load and strains in the middle plane of plate in specimen 1-1

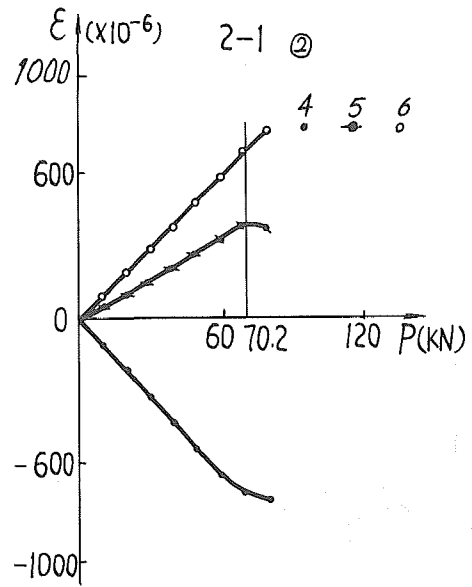


Fig. 5. c Load and strains in the middle plane of plate in specimen 2-1

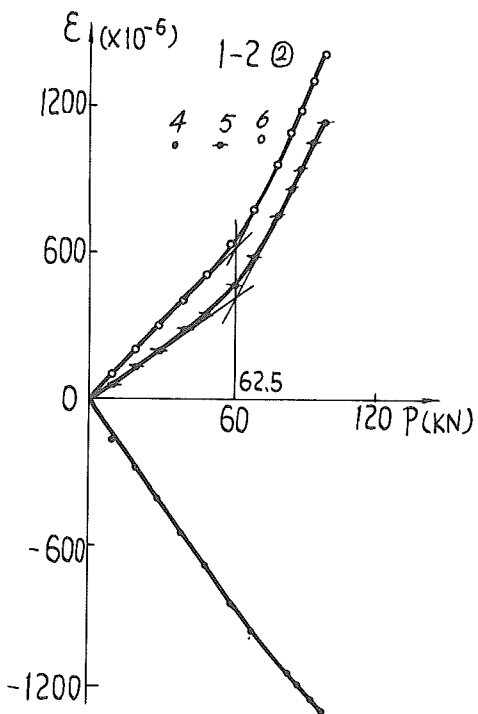


Fig. 5. b Load and strains in the middle plane of plate in specimen 1-2

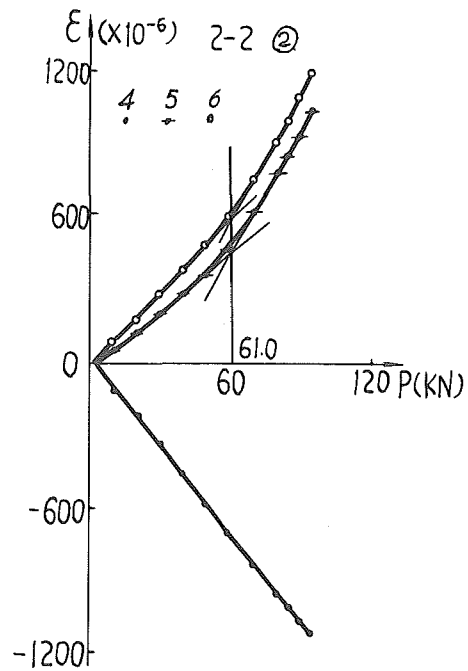


Fig. 5. d Load and strains in the middle plane of plate in specimen 2-2

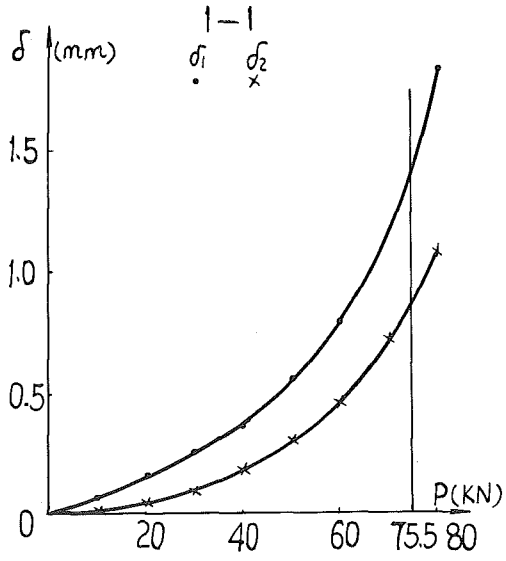


Fig. 7. a Deflections of plate at the measured points in specimen 1-1

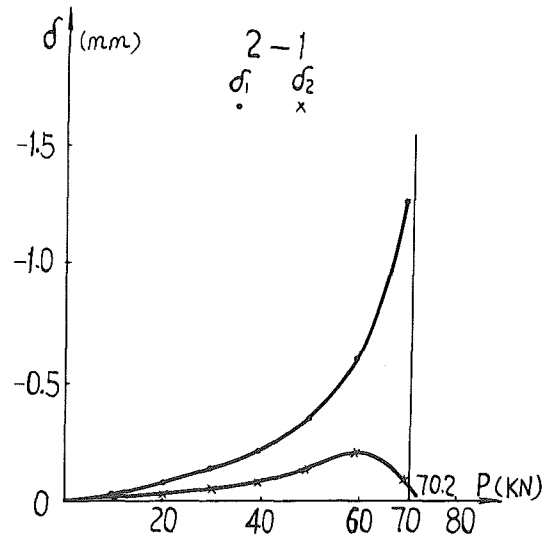


Fig. 7. c Deflections of plate at the measured points in specimen 2-1

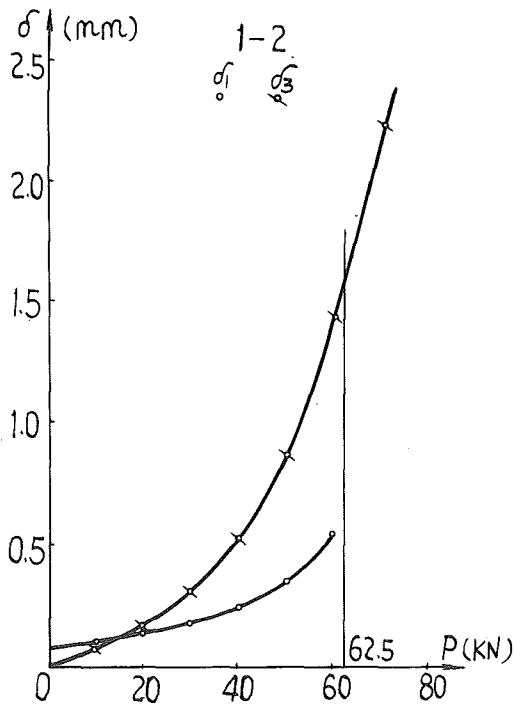


Fig. 7. b Deflections of plate at the measured points in specimen 1-2

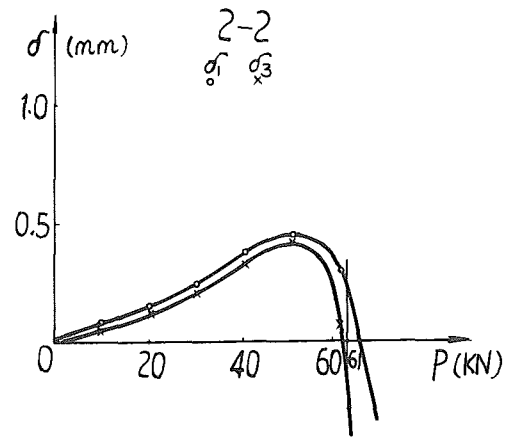


Fig. 7. d Deflections of plate at the measured points in specimen 2-2

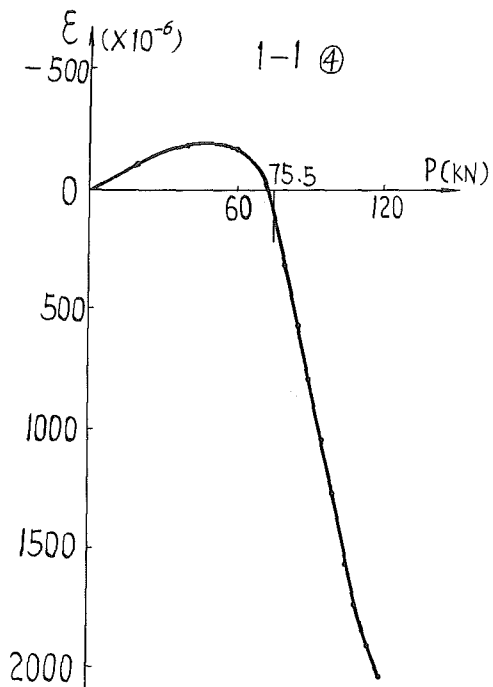


Fig. 6. a Load and strains in the stand-flange of stiffener in specimen 1-1

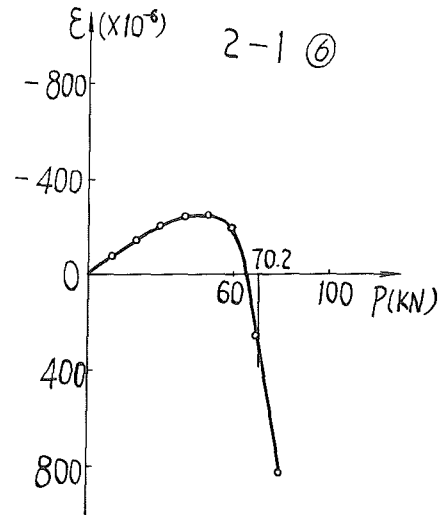


Fig. 6. c Load and strains in the stand-flange of stiffener in specimen 2-1

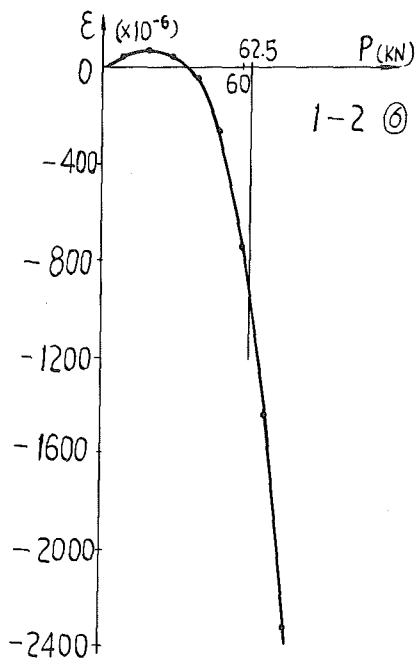


Fig. 6. b Load and strains in the stand-flange of stiffener in specimen 1-2

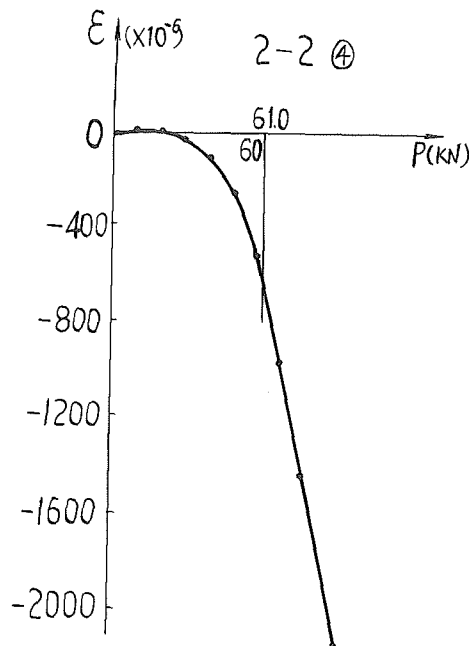


Fig. 6. d Load and strains in the stand-flange of stiffener in specimen 2-2

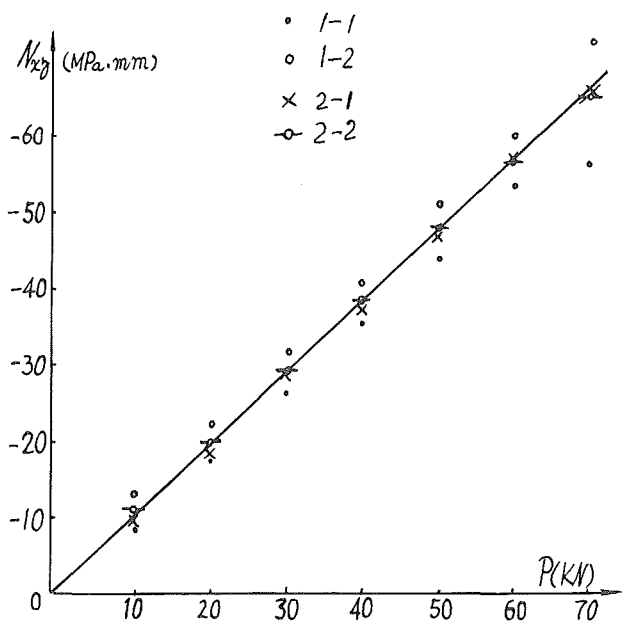


Fig. 8 Average test values of shear in all measured points

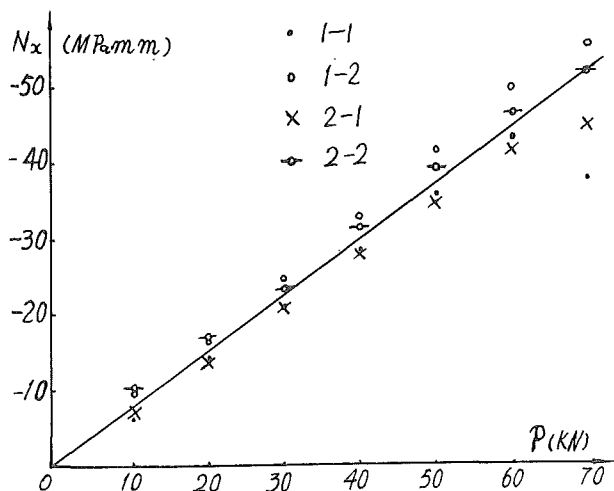


Fig. 9 Average test values of compression in all measured points

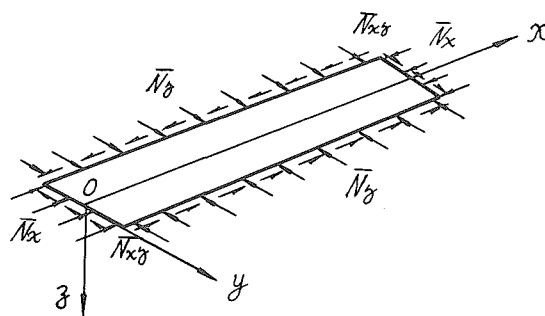


Fig. 10 Typical flat finite strip element subjected to combined inplane loads

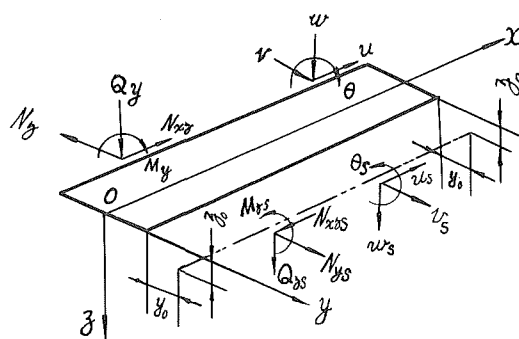


Fig. 11 Generalized displacements and forces at sides of strip, offsets of common intersection from side in reference plane

SPECIMEN NUMBER	LOAD WITH SUDDEN CHANGE OF STRAIN		LOAD WITH SUDDEN CHANGE OF DEFLECTION (kN)	BUCKLING LOAD(kN)		
	PLATE (kN)	STIFFENER(kN)		ANALYTICAL	TEST	RELATIVE DEVIATION
1-1	~80	~80	~80	68.05	75.5	10.9%
1-2	60~70	60~70	~70	68.05	62.5	-8.2%
2-1	~70	~70	~70	68.05	70.2	3.2%
2-2	60~70	60~70	60~70	68.05	61.0	-10.4%

Table 1. Test buckling load and comparison with the analytical value

SPECIMEN NUMBER	1-1				1-2				2-1				2-2			
	M. P. No	1	2	3	AV.	1	2	3	AV.	1	2	3	AV.	1	2	3
10.0	-136.0	-128.6	-134.0	-132.9	-129.9	-104.4	-120.6	-118.3	-130.6	-133.3	-130.5	-131.5	-103.0	-107.8	-108.5	-106.4
20.0	-123.4	-120.2	-125.4	-123.0	-137.0	-118.2	-129.8	-128.3	-134.1	-137.1	-134.3	-135.2	-115.0	-119.1	-117.2	-117.1
30.0	-126.1	-122.2	-128.3	-125.5	-136.3	-121.1	-130.5	-129.3	-134.5	-136.0	-133.8	-134.8	-119.7	-122.6	-119.2	-120.5
40.0	-121.8	-121.2	-128.2	-123.7	-136.4	-123.0	-131.3	-130.2	-133.3	-135.2	-133.4	-134.0	-121.9	-123.6	-120.1	-121.9
50.0	-121.4	-120.7	-126.9	-123.0	-135.2	-121.4	-128.7	-128.4	-135.4	-135.9	-134.4	-135.2	-122.2	-124.3	-120.2	-122.2
60.0	-120.8	-120.5	-126.6	-122.6	-137.6	-123.1	-130.8	-130.5	-139.2	-137.5	-136.4	-137.7	-122.2	-123.9	-120.2	-122.1
70.0	-122.2	-121.9	-126.6	-123.5	-145.2	-130.2	-139.6	-138.3	-142.4	-146.1	-154.9	-147.8	-127.6	-128.7	-121.7	-126.0
AV	-124.5	-122.2	-128.0	-124.9	-136.8	-120.2	-130.2	-129.0	-135.6	-137.3	-136.8	-136.6	-118.8	-121.4	-118.2	-119.5

A% = N_{xy}/N_x ; P, LOAD; M. P. No., THE NUMBER OF THE MEASURED POINT; AV., AVERAGE
Table 2 Test loads and the ratios between shear and compression at measured points (%)